


RESEARCH ARTICLE

Design and fabrication of a microfluidic system with embedded circular channels for rotary cell culture

Oihane Mitxelena-Iribarren^{1,2}  | Xabier Bujanda² | Laura Zabalza² | Janire Alkorta³ | Aitziber Lopez-Elorza³ | Raquel Gracia³ | Damien Dupin³ | Sergio Arana^{1,2} | Jesús Ruiz-Cabello^{4,5,6,7} | Maite Mujika^{1,2}

¹CEIT-Basque Research and Technology Alliance (BRTA), Donostia-San Sebastián, Spain

²Universidad de Navarra, Tecnun, Donostia-San Sebastián, Spain

³CIDETEC, Basque Research and Technology Alliance (BRTA), Parque Científico y Tecnológico de Gipuzkoa, Donostia-San Sebastián, Spain

⁴CIC biomaGUNE-Basque Research and Technology Alliance (BRTA), San Sebastián, Spain

⁵CIBER de Enfermedades Respiratorias (CIBERES), Madrid, Spain

⁶Ikerbasque, Basque Foundation for Science, Bilbao, Spain

⁷Universidad Complutense de Madrid, Madrid, Spain

Correspondence

Oihane Mitxelena-Iribarren, CEIT-Basque Research and Technology Alliance (BRTA), Manuel Lardizábal 15, 20018 Donostia-San Sebastián, Spain.
Email: oimixelena@ceit.es

Funding information

Basque Government, Grant/Award Number: KK-2019/00015

Abstract

The development of functional blood vessels is today a fundamental pillar in the evaluation of new therapies and diagnostic agents. This article describes the manufacture and subsequent functionalization, by means of cell culture, of a microfluidic device with a circular section. Its purpose is to simulate a blood vessel in order to test new treatments for pulmonary arterial hypertension. The manufacture was carried out using a process in which a wire with a circular section determines the dimensions of the channel. To fabricate the blood vessel, cells were seeded under rotary cell culture to obtain a homogeneous cell seeding in the inner wall of the devices. This is a simple and reproducible method that allows the generation of blood vessel models in vitro.

KEYWORDS

blood vessel, circular channels, microfluidic device, pulmonary hypertension

1 | INTRODUCTION

Pulmonary hypertension (PH) is a disease of the small pulmonary arteries that consists of cellular hyperproliferation and vascular remodeling.^[1] Although different biological (e.g., gene, protein, and metabolites) markers have been investigated for their diagnostic use in PH, one of the main problems investigating biomarkers for this disease is the low number of samples that researchers have in the studies, as lung biopsies are too invasive.^[2-7]

Given the need to open new lines of research in this disease, the use of microfluidic technology to simulate the pathological picture of this disease is an option that can lead to promising results in the treatment of PH. This technology can provide the possibility to evaluate new treatments for PH in vitro, and then extrapolate the results to a real environment with patients.

In recent decades, microfluidics has become a useful tool to simulate blood vessels in vitro and carry out pharmacological or therapeutic studies on them. The use of techniques such as soft-lithography to

This is an open access article under the terms of the Creative Commons Attribution-NonCommercial-NoDerivs License, which permits use and distribution in any medium, provided the original work is properly cited, the use is non-commercial and no modifications or adaptations are made.

© 2023 The Authors. *Biotechnology Journal* published by Wiley-VCH GmbH.

fabricate microfluidic devices with circular channels^[8] has allowed the cardiovascular system to be simulated with greater precision compared to traditional devices that presented rectangular channels.^[9] New elaborated photolithography techniques have been developed in order to obtain half-rounded vascular networks, as shown by Fenech et al. who developed a new single-mask photolithography process using an optical diffuser to produce a backside exposure leading to microchannels with both a rounded cross section and a direct proportionality between local height and local width, allowing a one-step design of intrinsically hierarchical networks.^[10] This is not the only technique used to obtain this type of channel. Methods such as the use of wires to reproduce circular tracks^[11,12] or the injection of liquid PDMS into rectangular channels and then air, to allow tubular devices to be obtained, have also been reported.^[13–15]

The main advantage of working with this type of device is that it enables the reproduction of the forces suffered by the blood when circulating through the vessels; this could not be achieved by rectangular channels.^[16] Other advantages of these devices are that, when working on a microscopic scale the surface tension forces dominate with respect to gravity, which are used to direct the flow without the need for external control. In addition, the reaction times are much shorter than on a macroscopic scale because diffusion occurs more quickly.^[17]

In order to mimic the structure of the blood vessels inside microfluidic devices, two types of cells such as endothelial cells and smooth muscle cells can be used: smooth muscle cells are located in the outermost area of the artery, while the endothelial cell layer is located in the inner site of the vessel. When fabricating these type of artificial vessels, the device usually undergoes a rotation, providing a dynamic seeding. On the one hand, manual rotary cell culture formations are based on the repeatedly seeding: after the seeding of cells performed in one position and ensuring the attachment of those cells, the device is manually rotated a specified number of degrees. After completing one whole lap and the cells seeded in each turn are attached, the device is incubated under static conditions.^[18] On the other hand, the orbital movement to ensure the cell culture is distinguished by selecting an orbital laboratory shaker that allows vertical and horizontal movements of the devices.^[19]

When blood vessels are formed in the device, new therapies can be tested. One of the promising therapies for PH is the use of nanopharmaceuticals that could reach the pulmonary vasculature rapidly and more efficiently than current therapies, as enhanced accumulation and persistence of nanoparticles has been observed in lungs undergoing PH following both intravenous and inhalational routes of delivery.^[20] In fact, nanotechnology provides means to design drug delivery systems that can transport drugs more effectively and improve releasing these on the chosen target. Delivery systems can be developed using nanostructures such as polymeric nanoparticles, lipid systems (i.e., liposomes and emulsions), carbon nanostructures such as nanotubes, and self-assembling micelles.^[21] Modified polysaccharides such as dextran methacrylate (DXT-MA) and dextran-based single chain nanoparticles (DXT-SCPNs) have been successfully used as oil-in-water nanoemulsions (O/W NEs) stabilizers to produce hydrophilic nanoparticles.^[22,23] These O/W NEs have demonstrated to be promising nanocarriers to

prolong the residence time of hydrophobic drugs in the lungs after inhalation.^[24]

In the present study, the main objective was the development of a microfluidic platform simulating the environment of the pulmonary arterial vasculature. For this, devices with tubular channels inside were designed and manufactured to mimic the environment of the vasculature. The *in vitro* model proposed for testing the effectiveness of the treatments developed is based on a cellular structure that recreates the inner part of the arterioles of the pulmonary arterial vasculature. The fabrication process of the tubular channels has been optimized and made easier in this study. In addition, once the device was fabricated and characterized, cells have been incubated using a novel custom rotary system, to guarantee the covering of the tubular walls. Then cytotoxicity of NEs designed to be inhaled by the patient was determined. In this way, it was identified that those nanomedicines would not damage the initial layer of endothelial cells on their way to their therapeutic target, the smooth muscle cells of the arterioles. More concretely, in this paper, the lack of toxicity of the different formulations over endothelial cells in a tubular microfluidic device is demonstrated. In fact, this research established a new microfluidics-based mechanism to mimic functional blood vessels and test the potential of more effective therapies for illnesses such as the PH.

2 | MATERIALS AND METHODS

2.1 | Fabrication and characterization of the microfluidic devices

The technique used to fabricate the circular channel microfluidic devices was a variant of the known microwire technique. First, in order to standardize the manufacture of devices, a mold was made by 3D printing. The mold was drilled on the sides with a drill bit through which the wire that would shape the channels was introduced and a glass was placed in the lower part to contain the polymer. Three-wire diameters were used in the process to obtain different diameters of the microfluidic channel: 0.12, 0.20, and 0.29 mm, in order to mimic the size of arterioles and small arteries.

The polymer used was PDMS, Sylgard 184, Dow Corning, with a 10:1 polymer to curing agent ratio, following the procedure described elsewhere.^[25] In a mixer, both components were added for 3 min and 30 s, without any degassing. After introducing the wire through the holes, the mold was sealed with parafilm and tape in order to avoid leaks. The polymer was then poured in and allowed to cure for 48 h at room temperature. Finally, the wire was extracted and each channel was cut into smaller devices (0.6–1.5 cm long).

In the characterization of the manufactured devices, four methods were used to analyze leaks, problems in the continuity of the channels and the topography of the internal wall of the same. The first method was based on the circulation of a dye through the channels using a dye, a syringe, and a connector. The second method used was optical, in which three microscopes were used: Leica M60, Nikon Eclipse Ti, and a Phenom G2 PRO-SEM scanning electron microscope from the Phenom

World brand. The Leica M60 microscope was used to determine the channel's continuity, by introducing several dyes and observing the color change in the inner tube with the microscope. In the second characterization method, following the protocol used in other works,^[26,27] fluorescent spheres were fixed on the wall of the devices. Using a Nikon Eclipse Ti fluorescence microscope, the inner surface of the channels was analyzed. Lastly, when using the SEM to determine the exact size of the inner tube of the microfluidic device, the sample had to be covered with a conductive material to be observed under the microscope. The coating process was carried out in a vacuum chamber Emitech (Kent, UK), where the sample was covered with gold by sputtering its surface.

2.2 | Fabrication of a rotary system for the cell fixation in the circular channels

To achieve the fixation of cells around the entire canal, a rotation or movement of the device is necessary. For this, the characterization of a motor was carried out, since it would allow us to know the relationship between the volts with which this engine would be fed and the revolutions per minute of the axis of rotation. The voltage with which the motor was supplied was varied, starting with 0.5 V and reaching 10 V, increasing the motor supply by 0.5 V in each step and measuring the value of the revolutions per minute of the shaft. This motor would provide several advantages over the current methods to attach cells in tubular devices. The motor guarantees the slow and constant movement of the device to ensure the distribution of the cells along the whole surface of the inner tube. In addition, there is no need for any user to adjust the position of the device during the rotation period, saving time, and avoiding user related changes.

Parallel to the development of the rotary system and due to its dimensions, an incubator was fabricated to accommodate both the motor and the microfluidic device arose. The cell incubation was developed with a portable isothermal container and using a temperature sensor and a humidity sensor. The temperature was controlled at constant 37°C inside the incubator through three rectangular 12 V-5 W heating mats, a digital thermostat and a PT-100 connected to Arduino. The mats were located at different points of the incubator to determine if the temperature was homogeneous in the whole volume. The normal procedure consisted of increasing the voltage applied to the heating mats, from 1 to 12 V, with a step of 1 V, and the temperature measured by both the PT-100 and the digital thermostat was recorded. Finally, with the same configuration as in the previous case, constant heating was carried out at 12 V in the three mats, and the time needed to reach the target temperature was calculated.

Regarding humidity control, two Petri dishes with water were used on the incubator floor, a DHT11 humidity sensor and an Arduino. Two tests were carried out: (1) the first consisted of analyzing the variation in humidity by varying the volts with which the heating mats were fed; (2) in the second, the incubator was heated to a constant 37°C and the evolution of humidity was measured at this temperature for 150 min.

2.3 | Cell culture and viability in circular channels

Following the literature,^[19,28] three different cell culture methods were used to ensure that the cells were attached through all the tube walls: manual rotation, orbital culture, and rotation by motor. The cell line used was EAhy926, a human endothelial cell line, cultured using DMEM cell culture medium, with 10% fetal bovine serum (FBS) + 1% penicillin/streptomycin (Life Technologies, GB).^[29] After trypsinization, the cells were introduced using connectors and syringes into the channels. Cell media was firstly circulated inside the devices in order to interact with the PDMS surface, providing an environment more prone to cell adhesion.^[30] Fifty microliters of cell suspension were introduced in the tubular channel, being the cell concentration between 4.5 and 10×10^5 cells mL⁻¹.

The three different culturing techniques were used to attach the cells around the circular tube. In the cell culture carried out using the manual rotation technique, 4 turns of 90° were made, being the incubation time of 2 h in each position. After completing a full turn (after 8 h of the manual rotation process), the devices were cultured statically overnight in an incubator at 37°C and 5% CO₂. In the so-called orbital cell culture (Figure 1A), the devices were placed for two h on a platform rocker set to 6 rpm inside an incubator set at 37°C and 5% CO₂, followed by a static culture in the same incubator.

Finally, in the motor culture method (Figure 1B,C), the same procedure followed with the commercial platform rocker was carried out, using the homemade rotary system (the one detailed in the previous section). The rotation of the stepper motor was also set at 6 rpm and the temperature was maintained at 37°C with a controlled humidity during the 2-h rotation. Following the procedure performed with the other two methods, once the rotation was finished, the devices were incubated overnight in static conditions in an incubator set at 37°C and 5% CO₂.

After the cell culture and the incubation of the devices overnight, cell viability tests were performed. Due to the low amount of liquid that the tubular microfluidic device could host, no MTT assay could be achieved, as it did not reach the minimum required by this test. Therefore, Trypan blue and Live/Dead kits were used to dye the cells. These were observed under the Nikon Eclipse Ti microscope, with which images were captured and afterward processed to count the cells using ImageJ image software, as described elsewhere.^[31]

2.4 | Nanoemulsion effect over cells in a rotary tubular channel

As mentioned earlier, the *in vitro* model proposed in this study for testing the effectiveness of the treatments against PH is based on a cellular structure that mimics that of the arterioles of the pulmonary arterial network. In this task, the main objective was to observe how the nanoparticles affected the endothelial cells of the inner layer of the vasculature. The goal of nanoparticles is to penetrate the smooth muscle cell layer located in the outermost area of the artery without

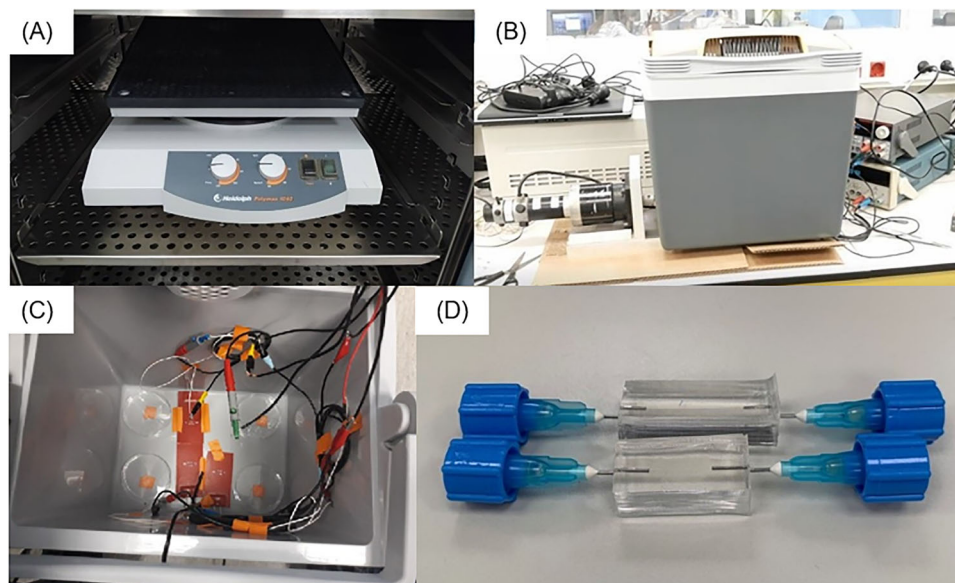


FIGURE 1 (A) “Orbital cell culture system”, which consisted of a platform rocker inside a cell incubator. (B) “Homemade rotary system”: rotation motor (left) attached to the incubator (middle) to enable continuous rotary cell culture. (C) Inside of the custom incubator containing the heating mats controlled by Arduino UNO. (D) Tubular microfluidic devices of different lengths with the connectors.

TABLE 1 Properties of the emulsions used in the study.

Name	Stabilizer	Crosslinker	Size (DLS)/PDI
A	DXT-SCPNs	Yes	284/0.2
B	DXT-SCPNs	No	307/0.2
C	DXT-MA	No	290/0.3
D	DXT-MA	Yes	259/0.2

DXT-MA, dextran methacrylate; DXT-SCPN, dextran based single chain nanoparticle.

damaging the inner endothelial layer. Thus, the effect they have on the EAhy926 cell line was verified in this study.

Different O/W NEs, obtained via sonication using sunflower oil, were studied to compare the effect on the endothelial cells of the NEs prepared with two different stabilizers (DXT-MA or DXT-SCPNs) (Table 1).

In addition, the effect of crosslinking the stabilizer, via thiol-Michael addition reaction using 2,2-(ethylenedioxy)diethanethiol to improve their long-term stability, was also investigated. The particle size of the different O/W NEs was measured by DLS and no significant differences were observed between the different NEs produced. In order to be able to test the nanoparticles on the cells, precise dilutions in the range of 10 and 1000 $\mu\text{g mL}^{-1}$ were prepared for the different tests.

Once the cells were incubated in the presence of the different types of nanoparticles for 72 h, under no rotation (because this was used to ensure cell attachment on the tubular channel walls), cell viability was obtained performing the Live/Dead fluorescence assay. For that, the commercial kit was added to the devices, which were observed under a Nikon Eclipse Ti microscope, with a high-resolution monochrome Hamamatsu camera and a specific stage that allowed temperature

control environmental conditions (37°C and 5% CO₂). The live cell population was then calculated using ImageJ software.

2.5 | Statistical analysis

For the statistical analysis, independent Student's *t*-test (or its non-parametric equivalent test) was performed to compare the inner diameter of the channels fabricated with the same wire, the effect of the different cell culture methods and the nanoparticles over cell viability. All the experiments were performed at least in triplicate and the values presented in the graphs are presented as the mean value \pm standard deviation.

The statistical significance criterion was the same for all the analyses. Statistical difference was determined as not significant (p -value > 0.05), significant (0.01 < p -value < 0.05), very significant (0.001 < p -value < 0.01), or extremely significant (p -value < 0.001).

3 | RESULTS AND DISCUSSION

3.1 | Fabrication and characterization of the microfluidic devices

The fabrication of the devices using the mold fabricated by 3D printing facilitated the PDMS fabrication process and ensured the reproducibility of the channels. The devices fabricated using this technique were fabricated successfully, with a PDMS thick enough to be manipulated (Figure 1D). The inner wires were removed leaving a microfluidic device with a tubular shape. To insert the reagent, connectors were attached to the PDMS pieces in both ends.

The mold facilitated the fabrication of tubular microfluidic devices, obtaining mm-long straight channels, uniform and clear all along. The characterization techniques provided information on the functionality and geometry of the channels. In the first place, the analysis employing of dyes allowed to verify that no channel showed leaks or flow obstructions. Once the continuity of the channels was confirmed with the use of dyes, the internal surface of the channel was characterized by microscopy. This technique allowed us to verify that all the channels were straight and cylindrical. The next characterization consisted in the use of the SEM microscope to study the real dimensions and the internal surface of the channels. Two cuts were made to the devices: one, cross-sectional to the channel length, which allowed to observe visually the circular orifice of the canal and the other, which divided the canal along two equal parts to analyze its internal surface. For all the diameters (120, 200, and 290 μm), it was observed that the dimensions of the channels were very similar to the wire diameter used for the fabrication (Figure 2A–F). However, in the case of the thinnest channels (120 μm) did not form a homogeneous cylindrical shape, changing the diameter of the inner tube along the device, probably due to the wire breaking during the demolding process. Therefore, the devices with the smallest diameters were discarded for further analyses. All the characterization techniques applied to the analysis of the quality of the channels provided enough information to determine that the fabrication process was reproducible, as the maximum deviation in the inner diameter of the devices differed less than a 5% from the target diameter for the three fabricated sizes ($n > 20$). Even more, no statistical difference was observed between the diameter size of the different devices fabricated with the same wire when performing the *t*-test (p -value < 0.05), demonstrating the reproducibility and repeatability of the process. In the case of the internal surface, it was found that all the channels presented certain roughness due to the stress to which the polymer is exposed in the mold release, which was very similar in all the cases.

Finally, to corroborate the tubular shape of the channel and assess the adhesion capability of the internal surface of the tubular channels, the attachment capability of some fluorescent nanoparticles was evaluated. The results of the images of the channel wall were not definitive because, when working with a thicker object, the images had noise from the different layers. To solve this problem, one of the Nikon Eclipse Ti microscope options was used, consisting of establishing a fixed depth and preventing the images from being affected by light from other layers. As observed, the protocol used for fluorescent nanoparticle adhesion, demonstrated the tubular shape of the device (Figure 2G,H). Even more, it was demonstrated that those surfaces were prone to be adherent. Therefore, cells were inserted in the devices for their incubation.

3.2 | Fabrication of a rotary system for the cell fixation in the circular channels

The relationship between the volts supplied to the motor and the output revolutions per minute was obtained by graphically representing

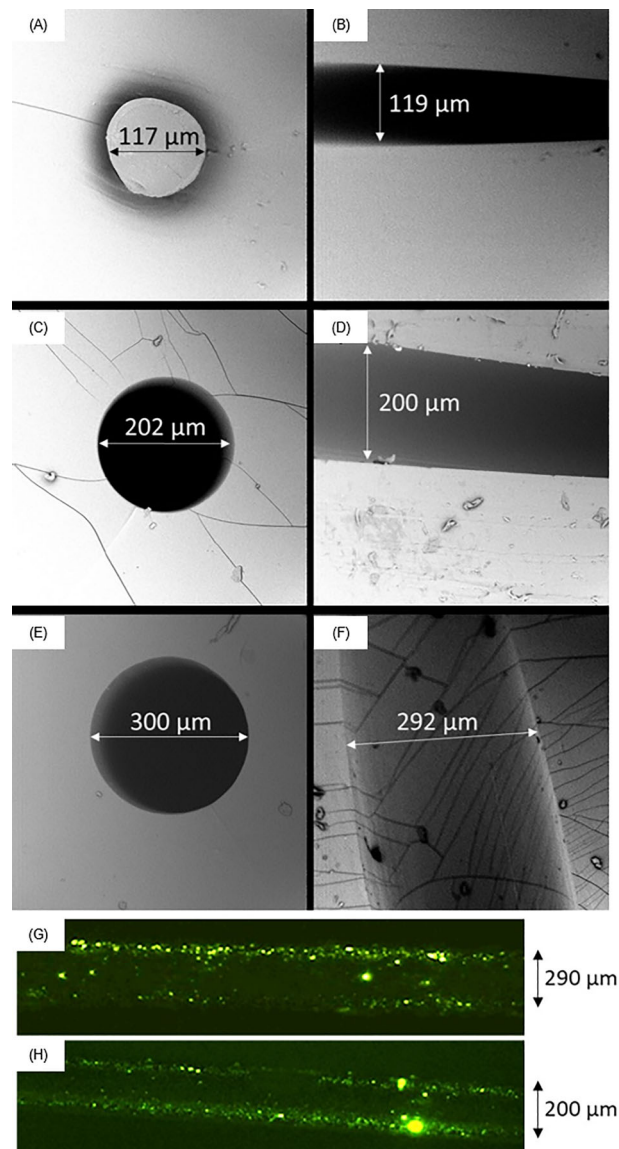


FIGURE 2 Images of the characterization of the channels manufactured using micro-molding by means of SEM (A–F) or fluorescent spheres (G, H). For the SEM images, the cross-section (A, C, E) and the longitudinal sections (B, D, F) of the channels can be observed. Three different channel diameters were fabricated: 0.12 mm (A, B), 0.20 mm (C, D), and 0.29 mm (E, F). In the images of the characterization performed by fluorescent spheres, a longitudinal section of the channels with a diameter of 0.29 mm (G) and 0.20 mm (H) are presented.

these results. A linear equation was obtained that made it possible to control the rotation of the shaft by varying the voltage.

Regarding the temperature control, 37°C was maintained within the incubator after 46 min. In addition, to achieve this temperature, the heating mats had to be constantly powered with 12 V. The sensor used to monitor the humidity in the chamber was not robust enough to measure under the established environmental conditions. Nevertheless, the success achieved by cell culturing in the customized incubator per-

formed afterwards demonstrated that the system provides sufficient humidity conditions for the cells to grow.

3.3 | Cell culture in circular channels

Following the literature,^[30] prior to introducing the cell suspension, cell media was firstly circulated inside the devices for 3 h to allow for the passive adsorption of serum proteins in the PDMS surface, providing an environment more prone to cell adhesion. Next, the cells were seeded and let to grow on the walls of the microfluidic devices (with an inner diameter of 200 and 290 μm) using the motored rotary system inside the homemade incubator.

To optimize the cell concentration to cover the entire device and attachment procedures to evaluate them, different trials were performed. The optimal length of the device for these tests was also determined. Thus, different concentrations of cells (0.5–1 million cells mL^{-1}) were inserted inside tubular devices of different lengths (0.6–1.5 cm). Their attachment was driven manually, by orbital rotation or using the motor plus incubator system.

The results of cellular attachment to the cylindrical structure obtained using the manual rotation technique showed that, with higher cell concentrations, their probability to attach to the walls of the channels was greater. However, these cells were not evenly distributed through the channel and remained localized in sections forming clumps. Due to clusters, the cells could not be counted. For this reason, this method was discarded for the rest of the experiments. When using the same cell concentration and conditions, such as the length of the device, the customized rotary system demonstrated a higher cell growth efficiency than the orbital method in all the different concentrations. In the latter, some cells agglomerated inside the tubular device and ended up having a rounded shape, which indicated that these adherent cells did not attach to the surface and died inside the tubular device after some hours (Figure 3A). The fact that cells did not attach to the channel surface was further supported by the fact that the insertion of dyes through the channel removed away those cells, corroborating that they were not properly attached to channel walls. On the other hand, the results turned out to be different in those devices in which the custom rotary system was used. The cells were evenly distributed throughout the prototype and adhered to the surface, which allowed them to grow (Figure 3B). This difference was further supported when performing the statistical analysis (Figure 3C), where a significant difference was observed between both fixation methods for the first two days (p -values < 0.05) and even an extremely significant difference after 72 h (p -value = 3×10^{-5}). The effect over the cells observed in the orbital method could be due to the movement that the commercial rocker provides. In this case, the liquid containing the cells inside the tubular devices does not fully turn covering all the walls, as it does in the case of the motored rotary system. This different movement could be the reason why the cells did not attach in the same way for both rotation methods, as the custom rotary systems guarantees the cell containing liquid touching all the circular surface of the channels, without letting them deposit mainly in one side.

Secondly, the appropriate concentration of cells to incubate in this type of device was determined. For this, the concentration of cells was seeded in a range of 4.5×10^5 – 10×10^5 cells mL^{-1} . In this case, when the initial cell concentration increased, a greater number of attached cells was observed after 2 h of rotation. In addition, the cells were distributed throughout the entire tubular structure. As observed in Figure 3D, they were attached to the walls of the tube, even after introducing the dyes. In fact, when focusing the image in the microscope, cells were well focused according to the side of the wall that was being focused. According to the cells counted in the platform (Figure 3E), it was determined that to ensure a cell amount enough to cover the entire device, a minimum initial concentration of 8×10^5 cells mL^{-1} was required. The statistical analysis performed showed a significant difference with respect to the lowest concentration from the beginning. As the incubation hours increased, it was determined that the initial cell concentration that showed the higher amount of attached living cells was 9×10^5 cells mL^{-1} , with a very significant difference with the other concentrations (p -values < 0.01).

Thirdly, the effect of the length of the devices on the growth of the cell layer was determined. To do this, the cell concentration was set at 9×10^5 cells mL^{-1} , and devices of two different lengths were used: 0.6 and 1.5 cm. A more extensive and homogeneous layer of cells was obtained throughout the entire device when introducing the same number of cells in a smaller space. In this way, it was determined that the length of 0.6 cm was more adequate for these devices (Figure 4A–D). Even more, when analyzing the cell population during time, a very significant difference (p -value = 2.5×10^{-3}) was obtained between the two lengths when reaching the 72 incubation hours.

3.4 | Nanoemulsion effect over cells in a rotary tubular channel

As mentioned before, one of the objectives of this work was to build an in vitro vascular model that could help to evaluate the degree of penetration of nanopharmaceuticals in a multilayer cell structure. These treatments need to pass through the endothelial layer without causing any damage and mostly reach the vascular smooth muscle cells of the outer layer of the artery.

To test the effect of the O/W NEs on the endothelial cells (EAhy926 cell line) was seeded and incubated for 24 h to ensure adhesion to the surface. After seeding the cells and incubating them, the different nanoparticles were introduced. After 72-h incubation time, the fluorescence was measured to obtain a semi-quantitative method to determine the viability of the endothelial cells in the presence of the different formulations. The number of live cells was determined using a commercial Live/Dead kit and a Nikon Eclipse Ti microscope, with a high-resolution monochrome Hamamatsu camera and a specific stage which allowed the control of temperature and environmental conditions (37°C and 5% CO_2). Cells showing fluorescence were quantified using ImageJ software. In this case, all the treatments used showed no toxicity to the endothelial cells, since the cell concentration remained stable even when the concentration of the emulsions and nanoparti-

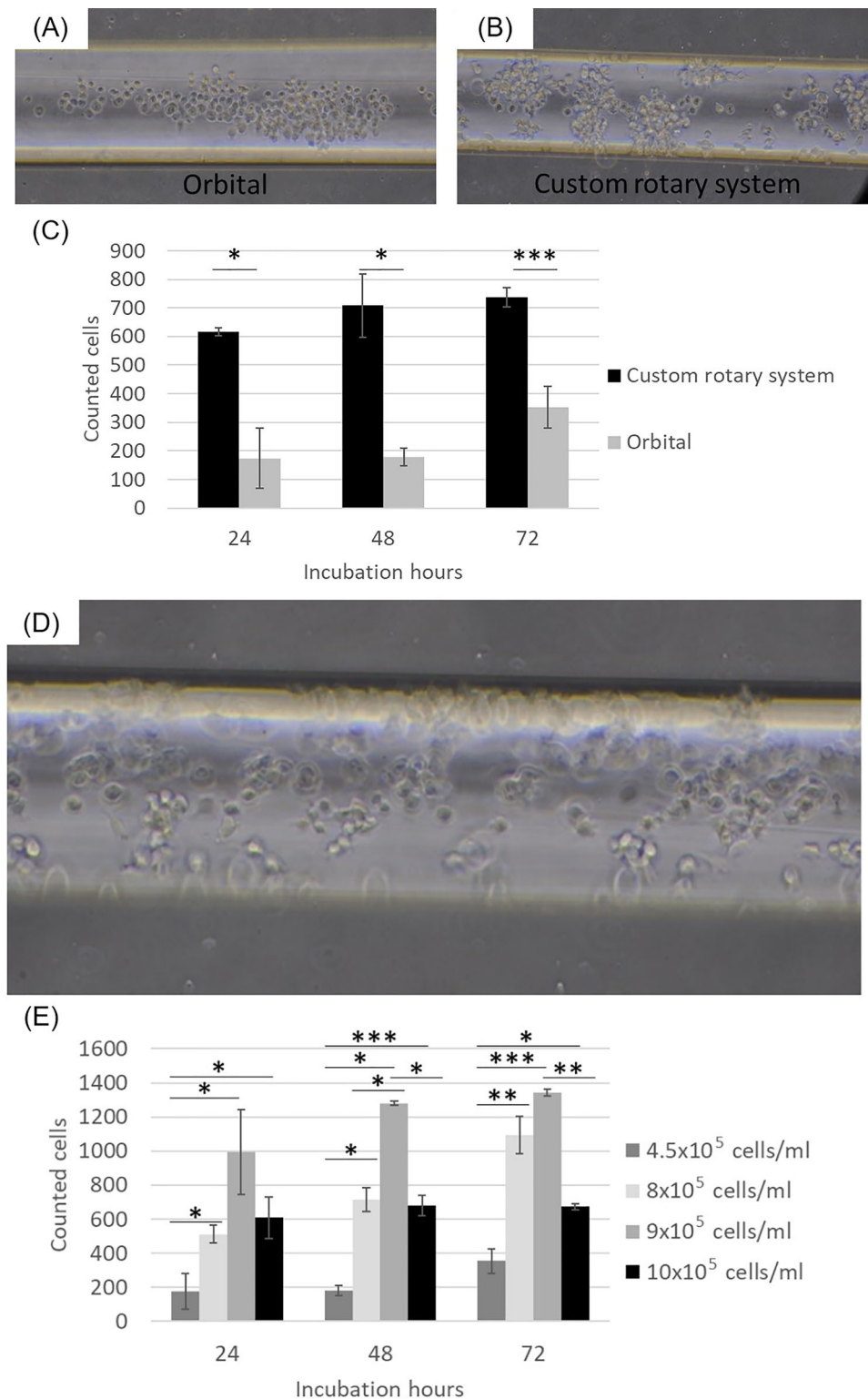


FIGURE 3 Cells inside tubular devices ($d = 200 \mu\text{m}$) after 24 h of incubation using (A) the orbital and (B) the custom rotary system. (C) Quantification of counted living cells over time when analyzing the effect of the fixation system (custom rotary system vs. orbital system), introducing an initial cell concentration of 4.5×10^5 cells mL^{-1} in a 1.5 cm long device. The statistical significance is shown in the graph as follows: significant (* p -value = 0.015 and 0.02) and extremely significant (** p -value = 2.76×10^{-5}). (D) Cells (inserted with an initial concentration of 8×10^5 cells mL^{-1}) in a tubular device ($d = 200 \mu\text{m}$) after 24 h of incubation. It can be seen that there are cells out of focus, since they are stuck along the tubular wall and they are in another plane of focus. (E) Quantification of counted living cells over time when analyzing the effect of cell concentration in 1.5 cm long devices using the custom fixation system. The statistical significance is shown in the graph as follows: significant (* $0.01 < p$ -values < 0.05), very significant (** $0.001 < p$ -values < 0.01) and extremely significant (** p -values < 0.001). Sample size for each cell incubation system, cell concentration and time point is ($n = 4$).

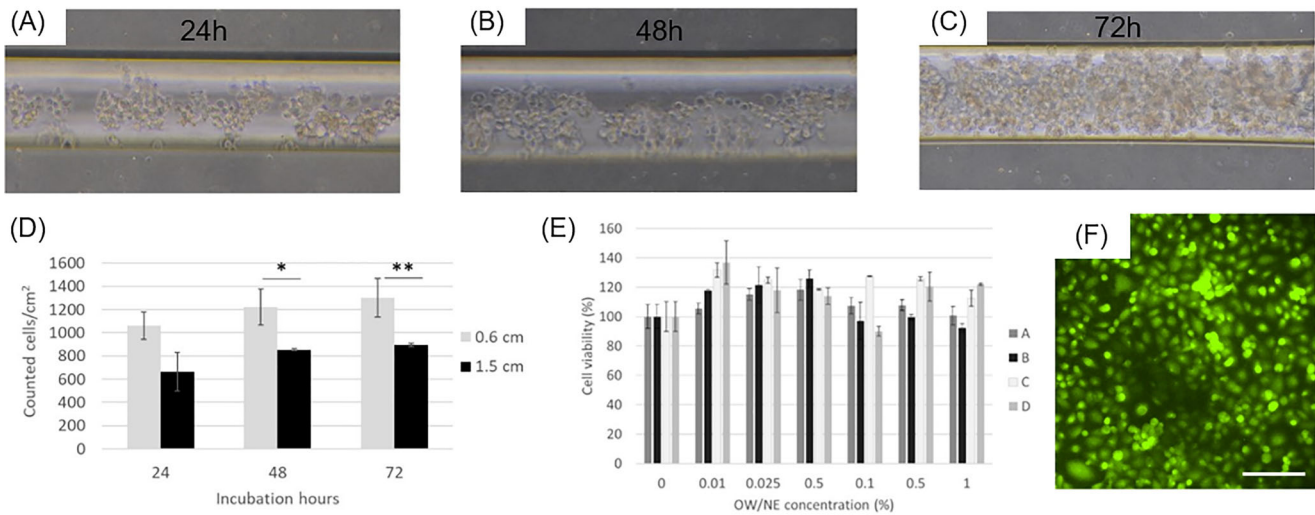


FIGURE 4 Cells (inserted with an initial concentration of 9×10^5 cells mL^{-1}) in a 0.6 cm tubular device ($d = 290 \mu\text{m}$) after incubating for (A) 24 h, (B) 48 h, and (C) 72 h. (D) Quantification of counted living cells over time when analyzing the effect of the length of the device when introducing 9×10^5 cells mL^{-1} . The statistical significance is shown in the graph as follows: (* p -value = 0.02) and very significant (** p -value = 2.5×10^{-4}). Sample size for each device length and time point is ($n = 4$). (E) Viability of endothelial cells in the presence of different oil-in-water nanoemulsions (O/W NEs) at different concentrations after 72 h of incubation. Sample size for each concentration is ($n = 4$). (F) Fluorescence image (showing live cells) obtained after 72 h of incubation of the endothelial cells in the presence of O/W NE A at its highest concentration ($n = 3$ for each O/W NE and concentration). Scale bar: $200 \mu\text{m}$.

cles was increased. Proof of this are the graph and the fluorescence image presented below (Figure 4E,F). It is worth mentioning that none of the O/W Nes tested showed a statistically significant decrease in cell population (p -values > 0.05).

4 | CONCLUSIONS

The fabrication of microfluidic devices with circular channels using the micro-wire technique allows the generation of devices with straight, circular channels, and without damage, as well as being a reproducible technique. The dimensional stability of this method is very high since the diameters measured in the SEM were equal to the diameters of the wires used in the fabrication process. The motor-incubator system used in this work was developed correctly and allowed to grow cells in a rotary manner with better results than using the orbital or manual system. This system incubator could have implications in low resource settings as well, as the acquisition of the materials used in the development of this system are cheaper than shaker and the commercial incubators. Regarding cell culture inside the tubular device, the following can be concluded: (1) the concentration of cells to be introduced into the devices is over 8×10^5 cells mL^{-1} , preferably 9×10^5 cells mL^{-1} ; (2) the use of channels with a shorter diameter favors the culture and gluing of cells in this type of channels; (3) the culture techniques that involve the custom rotary system developed in this study provided the best cell attachment; and (4) cells grow properly inside the tubular device during 72 h, increasing their growth nearly 30% by that time. Last but not least, different O/W NEs devel-

oped for the treatment of PH were tested over the endothelial cells. It was demonstrated that these treatments provoked no harm in the endothelial cell line. This establishes the groundwork for evaluating if these treatments will be able to cross this cell layer in healthy any proliferative conditions and then reach the smooth muscle cell layer, their therapeutic target.

AUTHOR CONTRIBUTIONS

Conceptualization: Damien Dupin, Sergio Arana, Jesús Ruiz-Cabello, and Maite Mujika; Data curation: Oihane Mitxelena-Iribarren; Formal analysis: Oihane Mitxelena-Iribarren, Xabier Bujanda, and Laura Zabalza; Funding acquisition: Damien Dupin, Sergio Arana, Jesús Ruiz-Cabello, and Maite Mujika; Investigation: Oihane Mitxelena-Iribarren, Xabier Bujanda, Laura Zabalza, Janire Alkorta, Aitziber Lopez-Elorza, and Raquel Gracia; Methodology: Oihane Mitxelena-Iribarren, Xabier Bujanda, Laura Zabalza, Janire Alkorta, Aitziber Lopez-Elorza, and Raquel Gracia; Project administration: Damien Dupin, Jesús Ruiz-Cabello, and Maite Mujika; Resources: Damien Dupin, Sergio Arana, and Maite Mujika; Software: Oihane Mitxelena-Iribarren, Xabier Bujanda, and Laura Zabalza; Supervision: Damien Dupin, Sergio Arana, Jesús Ruiz-Cabello, and Maite Mujika; Validation: Oihane Mitxelena-Iribarren, Xabier Bujanda, Laura Zabalza, Janire Alkorta, Aitziber Lopez-Elorza, and Raquel Gracia; Visualization: Oihane Mitxelena-Iribarren, Xabier Bujanda, and Laura Zabalza; Writing – original draft: Oihane Mitxelena-Iribarren; Writing – review & editing: Oihane Mitxelena-Iribarren, Xabier Bujanda, Laura Zabalza, Janire Alkorta, Aitziber Lopez-Elorza, Raquel Gracia, Damien Dupin, Sergio Arana, Jesús Ruiz-Cabello, and Maite Mujika.

ACKNOWLEDGMENTS

The authors would like to acknowledge the “Fundación contra la hipertensión pulmonar” (Empathy project). This work was funded by the Basque Government under the project KK-2019/00015 under the ELKARTEK 2019 call.


CONFLICT OF INTEREST STATEMENT

The authors declare no conflict of interest.

DATA AVAILABILITY STATEMENT

The data presented in this study are available on request from the corresponding author.

ORCID

Oihane Mitxelena-Iribarren  <https://orcid.org/0000-0002-7884-2430>

REFERENCES

- Galiè, N., McLaughlin, V. V., Rubin, L. J., & Simonneau, G. (2019). An overview of the 6th World Symposium on Pulmonary Hypertension. *The European Respiratory Journal*, 53(1), 1802148. <https://doi.org/10.1183/13993003.02148-2018>
- Román, J. S., Castillo Palma, M. J., García Hernández, F. J., & León, R. G. (2011). Marcadores biológicos. Utilidad para el control del paciente con hipertensión pulmonar. *Archivos de Bronconeumología*, 47, 21–25. [https://doi.org/10.1016/S0300-2896\(11\)70056-4](https://doi.org/10.1016/S0300-2896(11)70056-4)
- Kedzierski, P., & Torbicki, A. (2019). Precision medicine – the future of diagnostic approach to pulmonary hypertension? *Anatolian Journal of Cardiology*, 22(4), 168. <https://doi.org/10.14744/ANATOLJCARDIOL.2019.97820>
- Hemnes, A. R. (2018). Using omics to understand and treat pulmonary vascular disease. *Frontiers in Medicine*, 5, 157. <https://doi.org/10.3389/FMED.2018.00157>
- Hemnes, A., Rothman, A. M. K., Swift, A. J., & Zisman, L. S. (2020). Role of biomarkers in evaluation, treatment and clinical studies of pulmonary arterial hypertension. *Pulmonary Circulation*, 10(4), 1–17. <https://doi.org/10.1177/2045894020957234>
- Halliday, S. J., & Hemnes, A. R. (2017). Identifying “super responders” in pulmonary arterial hypertension. *Pulmonary Circulation*, 7(2), 300. <https://doi.org/10.1177/2045893217697708>
- Kan, M., Shumyatcher, M., & Himes, B. E. (2017). Using omics approaches to understand pulmonary diseases. *Respiratory Research*, 18(1). <https://doi.org/10.1186/S12931-017-0631-9>
- Chen, Y.-C., Chen, G.-Y., Lin, Y.-C., & Wang, G.-J. (2010). A lab-on-a-chip capillary network for red blood cell hydrodynamics. *Microfluidics and Nanofluidics*, 9, 585–591. <https://link.springer.com/article/10.1007/s10404-010-0591-6>
- Sato, K., & Sato, K. (2018). Recent progress in the development of microfluidic vascular models. *Analytical Sciences: The International Journal of the Japan Society for Analytical Chemistry*, 34(7), 755–764. <https://doi.org/10.2116/ANALSCI.17R006>
- Fenech, M., Girod, V., Claveria, V., Meance, S., Abkarian, M., & Charlot, B. (2019). Microfluidic blood vasculature replicas using backside lithography. *Lab on A Chip*, 19(12), 2096–2106. <https://doi.org/10.1039/C9LC00254E>
- Li, G., & Xu, S. (2015). Small diameter microchannel of PDMS and complex three-dimensional microchannel network. *Materials & Design*, 81, 82–86. <https://doi.org/10.1016/J.MATDES.2015.05.012>
- Jia, Y., Jiang, J., Ma, X., Li, Y., Huang, H., Cai, K., Cai, S., & Wu, Y. (2008). PDMS microchannel fabrication technique based on microwire-molding. *Chinese Science Bulletin*, 53(24), 3928–3936. <https://doi.org/10.1007/s11434-008-0528-6>
- Abdelgawad, M., Wu, C., Chien, W.-Y., Geddie, W. R., Jewett, M. A. S., & Sun, Y. (2011). A fast and simple method to fabricate circular microchannels in polydimethylsiloxane (PDMS). *Lab on A Chip*, 11(3), 545–551. <https://doi.org/10.1039/c0lc00093k>
- Nguyen, T. Q., & Park, W. T. (2016). Rapid, low-cost fabrication of circular microchannels by air expansion into partially cured polymer. *Sensors and Actuators B: Chemical*, 235, 302–308. <https://doi.org/10.1016/j.snb.2016.05.008>
- Kirchner, R., & Schiff, H. (2019). Thermal reflow of polymers for innovative and smart 3D structures: A review. *Materials Science in Semiconductor Processing*, 92, 58–72. <https://doi.org/10.1016/J.MSSP.2018.07.032>
- Truskey, G. (2004). *Transport phenomena in biological systems*. Pearson/Prentice Hall. <http://books.google.com/books?id=wuytQgAACAAJ>
- Convery, N., & Gadegaard, N. (2019). 30 years of microfluidics. *Micro and Nano Engineering*, 2, 76–91. <https://doi.org/10.1016/J.MNE.2019.01.003>
- van Engeland, N. C. A., Pollet, A. M. A. O., den Toonder, J. M. J., Bouten, C. V. C., Stassen, O. M. J. A., & Sahlgren, C. M. (2018). A biomimetic microfluidic model to study signalling between endothelial and vascular smooth muscle cells under hemodynamic conditions. *Lab on A Chip*, 18(11), 1607–1620. <https://doi.org/10.1039/C8LC00286J>
- Costa, P. F., Albers, H. J., Linssen, J. E. A., Middelkamp, H. H. T., van der Hout, L., Passier, R., van den Berg, A., Malda, J., & van der Meer, A. D. (2017). Mimicking arterial thrombosis in a 3D-printed microfluidic in vitro vascular model based on computed tomography angiography data. *Lab on A Chip*, 17(16), 2785–2792. <https://doi.org/10.1039/C7LC00202E>
- Segura-Ibarra, V., Wu, S., Hassan, N., Moran-Guerrero, J. A., Ferrari, M., Guha, A., Karmouty-Quintana, H., & Blanco, E. (2018). Nanotherapeutics for treatment of pulmonary arterial hypertension. *Frontiers in Physiology*, 9, 890. <https://doi.org/10.3389/FPHYS.2018.00890>
- De Silva, M. N. (2007). Nanotechnology and nanomedicine: A new horizon for medical diagnostics and treatment. *Archivos de La Sociedad Española de Oftalmología*, 82(6), 333–334. https://scielo.isciii.es/scielo.php?script=sci_arttext&pid=S0365-66912007000600002&lng=es&nrm=iso&tlng=es
- Navascuez, M., Gracia, R., Marradi, M., Díaz, N., Rodríguez, J., Loinaz, I., López-Gállego, F., Llop, J., & Dupin, D. (2021). Interfacial activity of modified dextran polysaccharide to produce enzyme-responsive oil-in-water nanoemulsions. *Chemical Communications*, 57(37), 4540–4543. <https://doi.org/10.1039/D1CC00819F>
- Gracia, R., Marradi, M., Cossío, U., Benito, A., Pérez-San Vicente, A., Gómez-Vallejo, V., Grande, H. J., Llop, J., & Loinaz, I. (2017). Synthesis and functionalization of dextran-based single-chain nanoparticles in aqueous media. *Journal of Materials Chemistry B*, 5(6), 1143–1147. <https://doi.org/10.1039/C6TB02773C>
- Navascuez, M., Dupin, D., Grande, H. J., Gómez-Vallejo, V., Loinaz, I., Cossío, U., & Llop, J. (2020). COSAN-stabilised omega-3 oil-in-water nanoemulsions to prolong lung residence time for poorly water soluble drugs. *Chemical Communications*, 56(63), 8972–8975. <https://doi.org/10.1039/D0CC00918K>
- Mitxelena-Iribarren, O., Hisey, C. L. L., Errazquin-Irigoyen, M., Gonzalez-Fernandez, Y., Imbuluzqueta, E., Mujika, M., Blanco-Prieto, M. J. J., Arana, S., González-Fernández, Y., Imbuluzqueta, E., Mujika, M., Blanco-Prieto, M. J. J., & Arana, S. (2017). Effectiveness of nanoencapsulated methotrexate against osteosarcoma cells: In vitro cytotoxicity under dynamic conditions. *Biomedical Microdevices*, 19(2). <https://doi.org/10.1007/s10544-017-0177-0>
- Mitxelena-Iribarren, O., Zabalo, J., Arana, S., & Mujika, M. (2019). Improved microfluidic platform for simultaneous multiple drug screen-

- ing towards personalized treatment. *Biosensors and Bioelectronics*, 123, <https://doi.org/10.1016/j.bios.2018.09.001>
27. Gomez-Aranzadi, M., Arana, S., Mujika, M., & Hansford, D. (2015). Integrated microstructures to improve surface-sample interaction in planar biosensors. *IEEE Sensors Journal*, 15(2), 1216–1223. <https://doi.org/10.1109/JSEN.2014.2361657>
28. Fiddes, L. K., Raz, N., Srigunapalan, S., Tumarkan, E., Simmons, C. A., Wheeler, A. R., & Kumacheva, E. (2010). A circular cross-section PDMS microfluidics system for replication of cardiovascular flow conditions. *Biomaterials*, 31(13), 3459–3464. <https://doi.org/10.1016/j.biomaterials.2010.01.082>
29. Lee, J. E., Patel, K., Almodóvar, S., Tuder, R. M., Flores, S. C., & Sehgal, P. B. (2011). Dependence of Golgi apparatus integrity on nitric oxide in vascular cells: Implications in pulmonary arterial hypertension. *American Journal of Physiology - Heart and Circulatory Physiology*, 300(4), H1141. <https://doi.org/10.1152/AJPHEART.00767.2010>
30. Hisey, C. L., Mitxelena-Iribarren, O., Martínez-Calderón, M., Gordon, J. B., Olaizola, S. M., Benavente-Babace, A., Mujika, M., Arana, S., & Hansford, D. J. (2019). A versatile cancer cell trapping and 1D migration assay in a microfluidic device. *Biomechanics*, 13(4). <https://doi.org/10.1063/1.5103269>
31. Mitxelena-Iribarren, O., Campisi, J., Martínez de Apellániz, I., Lizarbes-Sancha, S., Arana, S., Zhukova, V., Mujika, M., & Zhukov, A. (2020). Glass-coated ferromagnetic microwire-induced magnetic hyperthermia for in vitro cancer cell treatment. *Materials Science and Engineering: C*, 106, 110261. <https://doi.org/10.1016/j.msec.2019.110261>

How to cite this article: Mitxelena-Iribarren, O., Bujanda, X., Zabalza, L., Alkorta, J., Lopez-Elorza, A., Gracia, R., Dupin, D., Arana, S., Ruiz-Cabello, J., & Mujika, M. (2023). Design and fabrication of a microfluidic system with embedded circular channels for rotary cell culture. *Biotechnology Journal*, 18, e2300004. <https://doi.org/10.1002/biot.202300004>